ASIAN JOURNAL OF FORESTRY
Volume 10, Number 1, June 2026
Pages: 12

E-ISSN: 2580-2844
https://doi.org/10.13057/asianjfor/r100122

Comparative machine learning for forest landscape mapping in Mount Argapura, East Java, Indonesia

P. WIJAYATI WULANDARI[1], ENDANG HERNAWAN[2], ELHAM SUMARGA[2], ENDAH SULISTYAWATI[2,♥]

[1]Doctoral Program in Biology, School of Life Science and Technology, Institut Teknologi Bandung. Jl. Ganesa No. 10, Bandung 40132, West Java, Indonesia

[2]School of Life Science and Technology, Institut Teknologi Bandung. Jl. Ganesa No. 10, Bandung 40132, West Java, Indonesia.
Tel.: +62-22-251-1575, Fax.: +62-22-253-4107, ♥email: endah@itb.ac.id

Manuscript received: 21 October 2025. Revision accepted: 27 March 2026.

Abstract. *Wulandari PW, Hernawan E, Sumarga E, Sulistyawati E. 2026. Comparative machine learning for forest landscape mapping in Mount Argapura, East Java, Indonesia. Asian J For 10 (1): r100122. https://doi.org/10.13057/asianjfor/r100122.* Monitoring land cover is essential for understanding forest landscape structure and supporting sustainable management in mountainous regions. This study mapped land cover in the Mount Argapura landscape, East Java, Indonesia, using 2024 Landsat 8/9 imagery combined with topographic variables and topographic and texture metrics. Seven land-cover classes were identified: Natural Forest, Plantation Forest, Plantation Estate, Dryland Agriculture, Open Land, Settlements, and Water Bodies. Three machine-learning classifiers Classification and Regression Tree (CART), Random Forest (RF), and Support Vector Machine (SVM) were evaluated using Overall Accuracy (OA), Kappa (κ), 95% Confidence Intervals (CI), and McNemar's test. Results indicate that RF achieved the highest performance (OA=0.98; κ=0.97), significantly outperforming CART (OA=0.97; κ=0.96) and SVM (OA=0.87; κ=0.82). At the class level, RF showed high stability (User's Accuracy 0.98 for forest classes), while SVM struggled with spectral confusion between plantation and Dryland Agriculture. Spatial analysis reveals a landscape dominated by managed forest systems, with Plantation Forest covering 36.3% (35,544.33 ha) and Natural Forest covering 32.7% (32,043.51 ha). Together with Plantation Estates (22.1%), these vegetated classes account for over 91% of the 97,923.33 ha study area. Comparison with the official Indonesian Ministry of Environment and Forestry (MoEF) map showed moderate agreement (OA=0.54; κ=0.30), with this study identifying a larger extent of managed plantation landscapes (35,544.33 ha vs. 12,053 ha in MoEF). This discrepancy highlights the importance of local-scale mapping for capturing site-specific details. The findings provide a robust baseline for BKSDA and Perum Perhutani in biodiversity conservation, carbon stock assessment, and agroforestry planning. Future research should incorporate multi-temporal data to better detect fine-scale forest dynamics in this complex tropical terrain.

Keywords: Forest landscape, Landsat, land cover mapping, Mount Argapura, Random Forest

Abbreviations: BKSDA: CART: Classification and Regression Tree, CI: Confidence Interval, DA: Dryland Agriculture, DEM: Digital Elevation Model, FREL: Forest Reference Emission Level, GEE: Google Earth Engine, GIS: Geographic Information System, GLCM: Gray Level Co-occurrence Matrix, LULC: Land Use and Land Cover, MoEF: Ministry of Environment and Forestry, NBR: Normalized Burn Ratio, NDMI: Normalized Difference Moisture Index, NDVI: Normalized Difference Vegetation Index, NF: Natural Forest, OA: Overall Accuracy, OL: Open Land, PA: Plantation Area Estate, PF: Planted Plantation Forest, REDD+: Reducing Emissions from Deforestation and Forest Degradation, RF: Random Forest, SE: Settlement, SVM: Support Vector Machine, W: Water Bodies

INTRODUCTION

Land-use change is a primary driver of global environmental issues, severely impacting forest ecosystems and biodiversity. Recent studies show its impact is greater than previously estimated, affecting one-third of the Earth's land surface over the last 60 years (Winkler et al. 2021). LULC changes drive key forestry challenges deforestation, degradation, erosion, desertification, and biodiversity loss collectively undermining ecosystem stability and long-term sustainability (Velastegui-Montoya et al. 2022; Hanum et al. 2024). Human activities like agriculture and urban development now dominate landscape transformation, rapidly altering forests with enduring ecological consequences that far exceed natural disturbance (Dietz et al. 2023). These processes are most pronounced in tropical regions (Africa, SE Asia, and the Amazon), where deforestation and agricultural expansion drive biodiversity loss, hydrological disruption, and reduced carbon sequestration, weakening overall forest functions (Mahmoud et al. 2020; Bragagnolo et al. 2021; Slagter et al. 2024). Over time, these disturbances increase landscape instability, fire susceptibility, and soil degradation while reducing agricultural productivity. Collectively, these impacts challenge sustainable forest management and long-term resilience, especially under increasing anthropogenic pressure (Islam et al. 2023; Biah et al. 2024; Sovann et al. 2025). Accurate, up-to-date spatial LULC data is essential for monitoring forest conditions, assessing ecosystem services, and informed management. Remote sensing has emerged as the most efficient tool for mapping these changes across large, inaccessible areas (Tewabe and Fentahun 2020). Recently, LULC mapping has been increasingly integrated with GIS, enabling systematic

analysis of spatial patterns and landscape dynamics (Shah and Shah 2023). Among free datasets, Landsat 8/9 offers moderate resolution, multispectral capability, and a long-term archive, making it ideal for landscape-scale forest assessment and LULC monitoring (Roy et al. 2016). Landsat 8/9 data is widely applied to classify land cover types and support spatial analysis of ecosystem services and mapping (Shahfahad et al. 2023; Vatitsi et al. 2023). Advances in machine learning specifically algorithms like CART, RF, and SVM have enhanced remote sensing by handling large datasets and capturing non-linear spectral relationships in complex LULC mapping (Jozdani et al. 2019; Amin et al. 2024; Buthelezi et al. 2024). These machine learning techniques achieve higher classification accuracy in heterogeneous environments than traditional parametric classifiers. Recent Indonesian studies, such as in Sumedang Regency, demonstrate machine learning's efficacy; using Landsat 8, RF and SVM achieved high classification accuracies of 93.6% and 98.0%, respectively (Harmoko et al. 2025). Additionally, a comparison of five algorithms on Sentinel-2 data in Indonesian rural landscapes found RF yielded the highest overall accuracy at 98% (Trisasongko et al. 2022). These results demonstrate machine learning's effectiveness for LULC mapping in Java, indicating that multi-algorithm comparisons can reveal performance differences and gaps specifically in forested landscapes. Mount Argapura in East Java is a volcanic complex harboring some of the island's last tropical montane forest patches. These forests support high biodiversity, regulate regional climate, and provide crucial watershed protection and ecosystem services to local communities (Muhamad et al. 2014). Most forests in Mount Argapura are state-managed under various functions: conservation (Iyang Highlands Wildlife Reserve by *Balai Konservasi Sumber Daya Alam*/BKSDA), plus protection and production forests by Perum Perhutani. Recently, anthropogenic pressures notably agricultural expansion and settlement growth have accelerated land-use change, converting and fragmenting forests into agricultural and Open Land, thereby altering ecological functioning. (Guarderas et al. 2022). In this context, reliable land-cover information is critical for evidence-based forest management and conservation. This study compares the performance of CART, RF, and SVM classifiers for mapping the Mount Argapura landscape using 2024 Landsat 8/9 imagery, providing a baseline for analyzing land-use dynamics, carbon sequestration, and biodiversity conservation in this tropical montane region.

MATERIALS AND METHODS

Study area

The study area is Mount Argapura, East Java, Indonesia, spanning four districts (Jember, Probolinggo, Situbondo, and Bondowoso), and reaching a maximum elevation of 3,088 meters above sea level. The landscape comprises a complex mosaic of montane forest on the Iyang Plateau, managed forest estates, agroforestry zones, plantations, agricultural lands, and settlements across elevational gradients. Mount Argapura exhibits a highland climate that tends to resemble subtropical conditions with orographic influence, with an average annual rainfall of approximately 1,900 mm and temperatures generally ranging between 19-34°C, although temperature decreases with increasing elevation (Bimaprawira and Rejeki 2021). The variation in elevation and climatic conditions serves as a key determinant of vegetation types, hydrology, and land cover dynamics in the study area (Figure 1).

Procedures

Data collection

The image data were obtained from Google Earth Engine Catalog, a computing platform that enables users to perform geospatial analysis on Google's infrastructure and utilized ArcGIS Pro 3.5, a GIS software developed by the Environmental System Research Institute (Esri 2025). The properties of the Landsat 8/9 image used in this research are presented in Table 1.

Image processing and classification categories

This study implemented a systematic image processing workflow to ensure the accuracy and consistency of land cover classification results. The pre-processing stage included cloud and shadow masking using the Fmask algorithm integrated within the GEE pixel_qa band, along with the removal of sensor saturation.

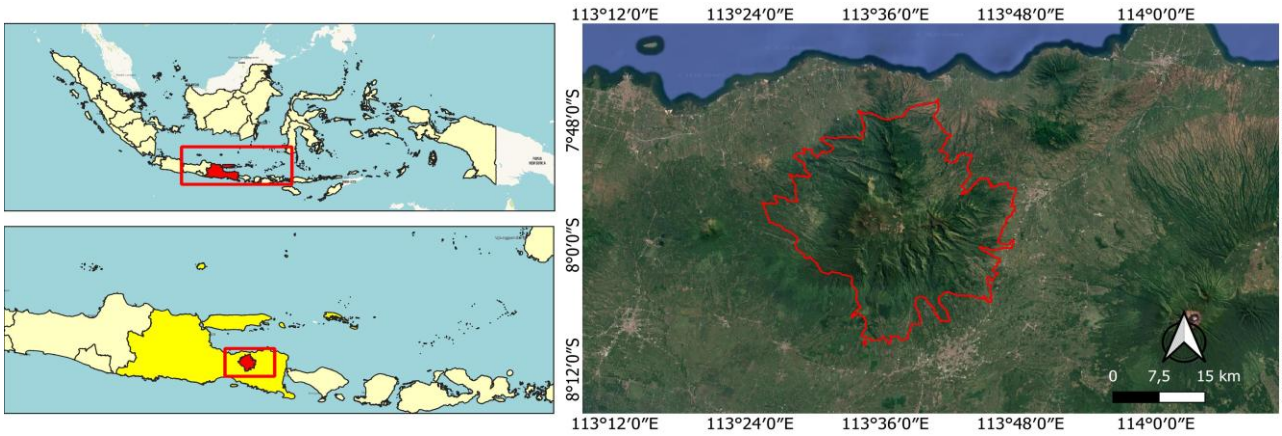

Figure 1. The location of the study area of Mount Argapura, East Java, Indonesia

Table 1. Properties of Landsat 8/9 imagery used in this study (Google Developers 2025)

	Properties
Product	USGS Landsat 8/9 Collection 2 Level-2 Surface Reflectance (SR)
Sensors	The Operational Land Imager Sensor (OLI) and The Thermal Infrared Sensor (TIRS)
Bands	Band 1 Coastal Aerosol (0.43 - 0.45 µm) 30 m Band 2 Blue (0.450 - 0.51 µm) 30 m Band 3 Green (0.53 - 0.59 µm) 30 m Band 4 Red (0.64 - 0.67 µm) 30 m Band 5 Near-Infrared (0.85 - 0.88 µm) 30 m Band 6 SWIR 1(1.57 - 1.65 µm) 30 m Band 7 SWIR 2 (2.11 - 2.29 µm) 30 m Band 8 Panchromatic (PAN) (0.50 - 0.68 µm) 15 m Band 9 Cirrus (1.36 - 1.38 µm) 30 m Band 10 TIRS 1 (10.6 - 11.19 µm) 100 m Band 11 TIRS 2 (11.5 - 12.51 µm) 100 m
Achieved at an altitude of	705 km
Field of view	185 km
Temporal resolution	16 days
UTM Zone	49 S
Path/Row	118/065, 118/066
Scene ID	LC09_L2SP_118065_20240819_20240819_02_T1 LC08_L2SP_117065_20240802_20240802_02_T1 LC09_L2SP_118066_20240717_20240717_02_T1 LC08_L2SP_117066_20240630_20240630_02_T1
Cloud Cover	6.32, 2.47, 3.85, 1.93 (%)
Data acquired	1 January to 31 December 2024
Band stacking	Multi-date composite imagery (median reducer)
Correction	the images have been atmospherically and terrain corrected using the built in processing provided in the SR products including Fmask-based cloud, shadow, cirrus, and snow masking, and terrain correction.
Pansharpening	No

All spectral bands were maintained at a uniform spatial resolution of 30 m. The final composite imagery was subsequently stacked with derived vegetation indices i.e. Normalized Difference Vegetation Index (NDVI), Normalized Burn Ratio (NBR), and Normalized Difference Moisture Index (NDMI) to enhance class separability and improve the accuracy of the land cover classification. NDVI measures vegetation greenness and health by comparing the reflectance of Near-Infrared (NIR) (which healthy vegetation strongly reflects) and red (RED) light (which vegetation absorbs for photosynthesis). The formula is:

NDVI=(NIR+RED)/(NIR-RED) (Rouse et al. 1974)

NBR is used to identify burned areas and burn severity. It contrasts NIR reflectance, which decreases after burning (due to vegetation loss), with SWIR reflectance, which increases (due to exposure of soil and char). Values closer to 1 represent healthy vegetation; lower or negative values represent burned or bare areas. The formula is:

NBR=(NIR+SWIR)/(NIR-SWIR) (Alcaras et al. 2022)

NDMI has the same mathematical form as NBR, but the interpretation differs because NDMI is used to measure vegetation water content, not burn severity. The formula is:

NDMI=(NIR+SWIR)/(NIR-SWIR) (Xu et al. 2025)

Values range from -1 to +1, where higher values indicate denser green vegetation. The stacked dataset is also enriched with topographic components such as DEM to obtain elevation and slope, which aid classification based on terrain conditions. Gray-Level Co-occurrence (GLCM) texture metrics, the statistical measures derived from image texture analysis such as contrast, homogeneity, entropy, and correlation (Tassi and Vizzari 2020) was incorporated to enhance class separability by providing additional surface pattern information for the classification process (Figure 2).

Training data were obtained from in 392 total training polygons across classes representing seven land cover classes: Natural Forest, Plantation Forest, Plantation Estate, dry land agriculture, settlement, Open Land, and Water Bodies (Table 2). The training samples were deliberately distributed across the study area to capture forest and non-forest heterogeneity, encompassing variations in canopy density, stand structure, land-use intensity, and landscape context. Natural and Plantation Forest samples included areas with differing vegetation densities and topographic settings, while non-forest classes represented a range of agricultural practices, settlement patterns, and degrees of land openness. These polygons were interpreted using very high-resolution basemap imagery available in Google Earth to ensure temporal and spatial consistency with the 2024 Landsat scenes (Ali et al. 2022). The training dataset was merged into a single feature collection and stratified by class to maintain balanced representation across land cover types (Yuh et al. 2023).

A stratified random sampling approach was then applied within Google Earth Engine (GEE) to divide the data into 70% for model training and 30% for accuracy testing (Shetty et al. 2021). Each sampled point was spatially independent, with a minimum separation distance of 60 meters to avoid spatial autocorrelation (Bogale et al. 2025). Cross-validation was not applied since an independent test subset was already used for accuracy assessment (Ramezan et al. 2019). The land cover class category used in the study refers to the land cover class used by Indonesian Ministry of Environment and Forestry (KLHK) in their Forest Reference Emission Level (FREL) document. FREL is the country's reference for measuring REDD+ emission reduction performance, including emissions reduction from deforestation, forest degradation, conservation role, sustainable forest management, and forest carbon stock enhancement (KLHK 2022).

Machine learning algorithm selection

The machine learning method used in this study is the supervised learning. The algorithm of the supervised learning was trained with labeled data to recognize patterns and predict results (Ouchra et al. 2023). This type of algorithm was used because it can handle complex data and generate accurate predictions. Three types of algorithms tested in this study were Classification and Regression Tree (Mahmoud et al. 2020), Random Forest (Melichar et al. 2023), and Support Vector Machine (Lemenkova 2024). The CART algorithm was configured with a minimum node split of 10, a maximum tree depth of 20, and a pruning Complexity Parameter (CP) of 0.01 (Demirović et al. 2022). The RF classifier was trained with 100 decision trees and employed the default number of predictor variables per split (√p). The SVM model utilized a Radial Basis Function (RBF) kernel with a penalty parameter (C) of 10 and γ = 0.1 (Yousefi et al. 2022). The selection of these three algorithms was motivated by the complexity of the seven land cover categories identified in the Mount Argapura imagery. Since each algorithm operates under distinct classification principles (Table 3), their comparative performance was evaluated to determine the most effective model for land cover classification in the study area.

Table 2. Description of land cover classes (and its Bahasa version) based on FREL (Boer et al. 2022)

Land cover classes	Abbreviation	Category
Natural Forest (*Hutan Alam*)	NF	Forest
Plantation Forest (*Hutan Tanaman*)	PF	Forest
Plantation Estate (*Perkebunan*)	PE	Non-Forest
Dry land agriculture (*Pertanian Lahan Kering*)	DA	Non-Forest
Open Land (*Lahan Terbuka*)	OL	Non-Forest
Settlement (*Pemukiman*)	SE	Non-Forest
Water Bodies (*Badan Air*)	W	Non-Forest

Table 3. Differences between algorithms used in the study (Valero and Alzate 2019)

Algorithm used	Working principle
Classification and regression tree	Building a single decision tree by recursively dividing the data based on the attribute value that yields the best results.
Random Forest	Building a decision tree randomly, then combining the results of many trees to make the final decision.
Support Vector Machine	Finding the optimal hyperplane to separate the data into two or more classes.

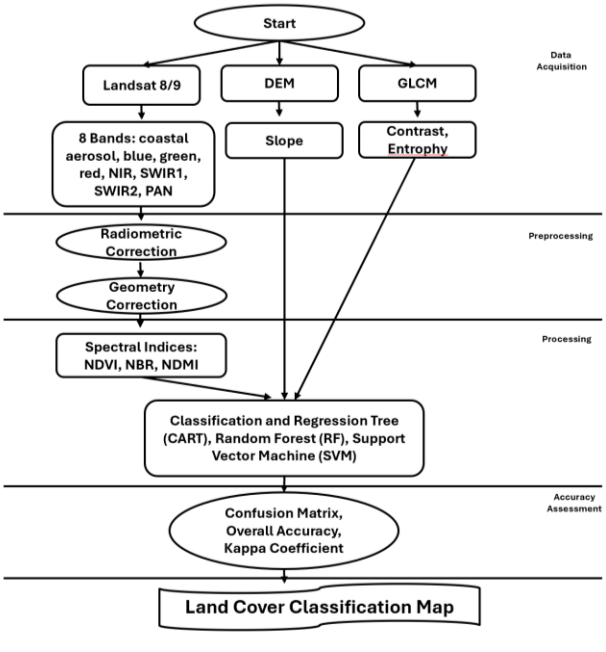

Figure 2. Steps involved in the Landsat 8/9 image processing to obtain the Mount Argapura land cover classification map

Data analysis

The accuracy assessment was conducted to quantitatively evaluate the performance of the land cover classification results generated by the three algorithms (Cheng et al. 2021). Accuracy assessment provides essential information on how well the classified map represents the actual land cover on the ground. The comparison between predicted and reference data was summarized in a confusion matrix, from which several statistical measures were derived, including Producer's Accuracy (PA), User's Accuracy (UA), Overall Accuracy (OA), and the Kappa Coefficient (κ).

Producer's Accuracy represents the probability that a reference pixel is correctly classified. It measures the omission error, which occurs when reference pixels of a given class are excluded from that class in the classification result. Mathematically, it is expressed as:

$$PA_i = \frac{n_{ii}}{\sum_{j=1}^{k} 1\, n_{ji}} \times 100\%$$

Where, n_{ii} is the number of correctly classified pixels for class *i*, and $\sum_{j=1}^{k} 1\, n_{ji}$ is the total number of reference pixels for class *i*. A low PA value indicates that many reference samples from class *i* were misclassified into other classes.

User's Accuracy quantifies the probability that a pixel classified into a given class actually represents that class on the ground. It reflects the commission error, which occurs when pixels are incorrectly included in a class. The formula is:

$$UA_i = \frac{n_{ii}}{\sum_{j=1}^{k} 1\, n_{ij}} \times 100\%$$

Overall Accuracy measures the proportion of correctly classified pixels among the total number of reference pixels. It provides a general indication of the classifier's performance and is computed as:

$$OA = \frac{\sum_{i=1}^{k} 1\, n_{ii}}{N} \times 100\%$$

Where, N is the total number of reference samples. While OA is a simple and widely used measure, it does not account for chance agreement between classes.

The Kappa statistic provides a more robust estimate of classification accuracy by adjusting for random agreement. It measures how much better the classification is compared to a random assignment of classes. The coefficient is calculated as:

$$\kappa = \frac{N \sum_{i=1}^{k} 1\, n_{ii} - \sum_{i=1}^{k} 1\, (n_{i+} \times n_{+i})}{N^2 - \sum_{i=1}^{k} 1\, (n_{i+} \times n_{+i})}$$

Where, n_{i+} and n_{+i} are the marginal totals for rows and columns of the confusion matrix, respectively. The κ value ranges from 0 to 1, where: $\kappa<0.40$ indicates poor agreement, $0.40\leq\kappa<0.75$ indicates moderate agreement, and $\kappa\geq0.75$ indicates strong agreement (Landis and Koch 1977). High κ values suggest that the classifier successfully distinguishes between different land cover types beyond random chance, thus providing higher confidence in classification outcomes.

Class-level uncertainty and confusion analysis were conducted to specifically evaluate the reliability of forest classes. In addition to overall accuracy metrics, a confusion matrix was used to derive Producer's Accuracy (PA) and User's Accuracy (UA) for each land-cover class, with particular emphasis on natural and Plantation Forests. This class-based assessment allowed identification of misclassification patterns between forest and spectrally similar non-forest classes, such as Plantation Estates and Dryland Agriculture. Evaluating accuracy at the class level is critical for forest monitoring applications, as it provides insight into thematic uncertainty and ensures that forest-related outputs are robust for ecological assessment and land management purposes (Congalton and Green 2005).

Statistical test

The reliability of differences in classification performance among algorithms was evaluated using two complementary statistical approaches: (i) estimation of the 95% Confidence Interval (CI) for overall accuracy through bootstrapping, and (ii) pairwise McNemar's test to assess the statistical significance between classifiers. These approaches enhance the robustness of the reported accuracies by quantifying uncertainty and determining whether one classifier performs significantly better than another (Foody 2020). The 95% Confidence Interval (CI) provide the range within which the true accuracy of a classifier is likely to fall with 95% confidence. Bootstrapping is a non-parametric resampling technique that repeatly samples (with replacement) from the validation dataset to estimate the variability of the accuracy metric.

If $\hat{p}$ denotes the observed accuracy from the validation data and $n$the number of validation samples, a simple binomial approximation of the CI is given by:

$$SE = \sqrt{\frac{\hat{p}(1-\hat{p})}{n}}$$

$$CI_{95\%} = \hat{p} \pm Z_{0.975} \times SE$$

Where, SE is the standard error and $Z_{0.975} = 1.96$ for a 95% confidence level.

In the bootstrap approach, the procedure is repeated B times (typically 1000), and the 2.5th and 97.5th percentiles of the resulting accuracy distribution define the lower and upper bounds of the CI:

$$CI_{95\%} = [\hat{p}_{(2.5)}, \hat{p}_{(97.5)}]$$

This approach does not assume normality and is suitable for any accuracy distribution.

The McNemar's test evaluates whether two classifiers differ significantly in their classification performance on the same dataset. It focuses on the number of samples that are classified differently by the two models. The McNemar's statistic is computed as:

$$\chi^2 = \frac{(|\, b - c\, | - 1)^2}{b + c}$$

Under the null hypothesis (no significant difference between classifier), χ^2 follows a chi-square distribution with I degree of freedom. If $\chi^2 > 3.84$ (corresponding to $p < 0.05$, the null hypothesis is rejected, indicating a significant difference the two classifiers.

The best land-cover map generated in this study was then compared against the national land-cover map provided by the Ministry of Environment and Forestry (MoEF). The comparative analysis focused on three primary classes: Natural Forest, Plantation Forest, and Plantation Estates, by measuring the extent of each category across both maps.

RESULTS AND DISCUSSION

Classification performances

The accuracy of the three algorithms' results was compared by their overall accuracy and the kappa index, estimation of the 95% Confidence Interval (CI) for overall accuracy, and McNemar's test to assess the statistical significance between classifiers. These can be seen in Tables 4 and 5.

Table 4. Confusion matrix results showing the accuracy of three machine learning tools

Land-cover	NF	PF	PE	DA	OL	SE	W	User_Acc
CART confussion matrix result								
NF	464	2	0	0	0	0	0	0.99
PF	2	475	4	12	0	2	0	0.96
PE	0	4	403	0	0	7	0	0.97
DA	0	18	0	31	0	0	0	0.63
OL	0	0	0	0	154	0	0	1
SE	0	0	2	0	0	68	0	0.97
W	0	0	0	0	0	0	4	1
Prod_Acc	0.99	0.95	0.99	0.72	1	0.88	1	0.97
RF confussion matrix result								
NF	465	1	0	0	0	0	0	0.99
PF	1	487	3	2	0	2	0	0.98
PE	0	5	408	0	0	1	0	0.99
DA	0	15	1	23	0	0	0	0.59
OL	0	0	0	0	154	0	0	1
SE	0	0	1	0	0	69	0	0.99
W	0	0	0	0	0	0	4	1
Prod_Acc	0.99	0.96	0.99	0.92	1	0.96	1	0.98
SVM confussion matrix result								
NF	447	2	0	0	0	0	0	0.99
PF	2	476	53	0	0	1	0	0.89
PE	8	90	279	0	0	3	0	0.73
DA	0	31	20	1	0	0	0	0.02
OL	0	0	0	0	160	0	0	1
SE	0	7	0	0	0	72	0	0.91
W	0	0	0	0	0	0	5	1
Prod_Acc	0.98	0.79	0.79	1	1	0.95	1	0.87

Note: NF: Natural Forest, PF: Plantation Forest, PE: Plantation Estate, DA: Dryland Agriculture, OL: Open Land, SE: Settlement, W: Water Bodies

Table 5. Overall accuracy, Kappa coefficient, 95% confidence interval (CI), and McNemar's test results

Model	Overall Accuracy (OA)	95% Confidence Interval	Kappa	McNemar Comparison	χ^2	p-value	Statistical Interpretation
CART	0.97	(0.96-0.98)	0.96	CART vs RF	8.76	0.003	RF significantly higher
				CART vs SVM	134.94	<0.001	CART significantly higher
RF	0.98	(0.97-0.99)	0.97	RF vs SVM	170.27	<0.001	RF significantly higher
SVM	0.87	(0.85-0.87)	0.82	-	-	-	Significantly lower accuracy

Note: CART: Classification and Regression Tree, RF: Random Forest, SVM: Support Vector Machine

Based on Table 4, Random Forest (RF) achieved the highest classification performance with an overall accuracy (OA) of 0.98 and a Kappa coefficient of 0.97, followed closely by CART (OA=0.97, Kappa=0.96), while SVM showed substantially lower performance (OA=0.87, Kappa=0.82) (Table 5). At the class level, RF produced consistently high producer's and user's accuracies for most land-cover types (≥0.96), particularly for Natural Forest (NF), Plantation Forest (PF), and Plantation Estate (PE). In contrast, SVM showed considerable misclassification between PF and PE, resulting in lower producer's accuracies for PF and PE (both 0.79) and extremely low user's accuracy for Dryland Agriculture (DA) (0.02). Although CART performed comparably to RF in several classes, its producer's accuracy for DA was lower (0.72) compared to RF (0.92).

Statistical comparison using McNemar's test (Table 5) confirmed that the performance differences were significant. RF performed significantly better than CART (χ^2=8.76, p=0.003) and SVM (χ^2=170.27, p<0.001), while CART also significantly outperformed SVM (χ^2=134.94, p<0.001). These results demonstrate that RF provides the most robust and statistically superior classification performance for forest landscape mapping in the study area.

The classification results were compared with the official MoEF reference map, resulting in an overall accuracy (OA) of 0.54 and a Kappa coefficient (κ) of 0.30, indicating a moderate level of agreement between the two maps. Data from the comparison between the best land-cover map generated in this study and the MoEF map, focusing on a comparative analysis of three primary classes

Natural Forest, Plantation Forest, and Plantation Estates are presented in Figure 3.

The classification map indicates a higher proportion of plantation-related land cover compared with the MoEF map. Plantation Forest constitutes the largest share in the classification results (36.3%), followed by Natural Forest (32.7%) and Plantation Estate (22.1%). In contrast, the MoEF map shows a dominant proportion of Natural Forest (49.4%), while Plantation Forest (15.3%) and Plantation Estate (5.6%) occupy substantially smaller areas. These differences suggest that the classification produced in this study identifies a larger extent of managed or cultivated forest landscapes, whereas the MoEF map represents a greater proportion of Natural Forest cover within the study area.

Land cover map

The spatial distribution of land cover types in Mount Argapura was effectively mapped using machine learning classification of Landsat 8/9 composite imagery with NDVI, NBR, NDMI, DEM, slope, and GLCM as predictors. The resulting maps (Figures 3) illustrate how CART, SVM, and RF classified the landscape. Meanwhile, the land-cover area estimated using the Random Forest algorithm is presented in Table 6.

Figure 4 presents a visual comparison of land-cover classification results generated using CART (Figure 4.A), RF (Figure 4.B), and SVM (Figure 4.C). Overall, the three maps show a broadly consistent spatial pattern, with forest-dominated classes concentrated in the central mountainous area and more heterogeneous land-cover types distributed toward the outer zones. Plantation Forest and Natural Forest visually dominate the landscape across all models, forming a continuous green belt in the core area, while Plantation Estate appears mainly in transitional zones surrounding the forest interior. However, noticeable differences emerge in the distribution of Settlement and Dryland Agriculture classes, particularly along the northern and peripheral areas. The RF map exhibits a more spatially compact and homogeneous classification pattern, whereas CART shows slightly more fragmented patches. In contrast, SVM presents greater class mixing in several boundary areas, indicating higher misclassification between plantation-related classes. These visual discrepancies reflect the differing sensitivity of each algorithm to spectral variation and landscape heterogeneity.

The land-cover composition indicates a strongly vegetated landscape dominated by managed forest systems. Plantation Forest represents the largest proportion of the study area (35,544.33 ha; 36.3%), followed by Natural Forest (32,043.51 ha; 32.7%) and Plantation Estate (21,648.87 ha; 22.1%). Together, these three classes account for more than 91% of the total area (97,923.33 ha), suggesting that the landscape is primarily characterized by forested and perennial plantation cover. In contrast, non-vegetated and built-up classes occupy relatively small proportions, with Settlement covering 4.9% (4,843.71 ha) and Open Land 3.5% (3,408.57 ha), while Dryland Agriculture (0.4%) and Water (0.03%) represent marginal components. Qualitatively, the dominance of Plantation Forest over Natural Forest suggests a shift toward more intensively managed forest systems rather than intact natural stands. Although no temporal comparison is presented in this table, the relatively large extent of plantation-based land use implies increasing anthropogenic influence within the forest landscape.

A comparison between the best-performing land-cover map produced using the Random Forest algorithm and the MoEF land-cover map reveals poor to moderate agreement between the two datasets. For example, this study identifies 32,043.51 ha of Natural Forest, whereas the MoEF map identifies 39,036 ha. For Plantation Forest, the classification map estimates 35,544.33 ha, while the MoEF map reports 12,053 ha. Similarly, Plantation Estate covers 21,648.87 ha in the classification map compared with 4,425 ha in the MoEF map. The remaining land-cover categories, Dryland Agriculture, Open Land, Settlement, and Water, are aggregated as other land-use classes, totaling 8,686.62 ha in the classification map and 23,509 ha in the MoEF map.

Table 6. Area of different land cover classes derived from the Random Forest classification of Mount Argapura, Indonesia

Land-cover class	Area (ha)	Area (%)
Natural Forest	32,043.51	32.7
Plantation Forest	35,544.33	36.3
Plantation Estate	21,648.87	22.1
Dryland Agriculture	405.72	0.4
Open Land	3,408.57	3.5
Settlement	4,843.71	4.9
Water	28.62	0.0
Total	97,923.33	100

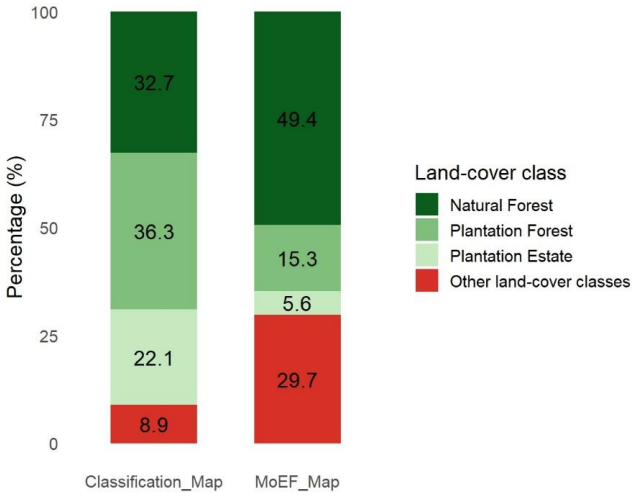

Figure 3. Comparison of land-cover class composition between the classification map produced in this study and the official MoEF map

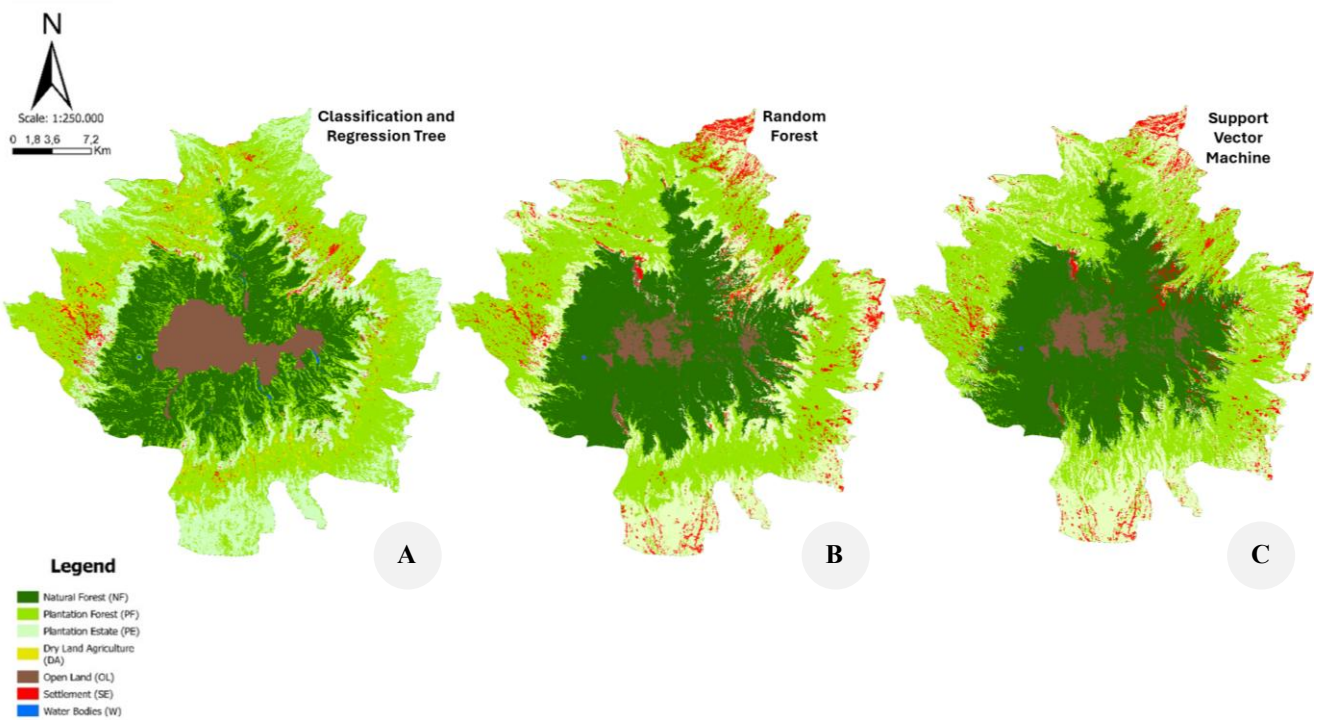

Figure 4. Comparison of land-cover classification results using: A. Classification and Regression Tree (CART), B. Random Forest (RF), and C. Support Vector Machine (SVM)

Discussion

Classification accuracy and uncertainty

The comparative analysis demonstrates that the RF algorithm achieved the highest classification accuracy, followed by CART and SVM. This result indicates that RF produces more detailed and stable land-cover classifications and exhibits a stronger capacity to capture complex spatial and spectral patterns than the other tested algorithms. The achieved accuracy levels are consistent with established benchmarks in remote sensing studies, where Kappa values above 70% are considered acceptable, above 80% reliable, and values exceeding 85% highly accurate for land-cover mapping applications (Anderson 1976; Carletta 1996; Sari et al. 2021). The classification of seven land-cover classes Natural Forest, Plantation Forest, Plantation Estate, Dryland Agriculture, Settlements, Open Land, and Water Bodies posed substantial challenges, as not all algorithms were equally successful in assigning pixels to their correct categories. This outcome reflects the inherent complexity of multi-class classification in heterogeneous tropical landscapes, where overall accuracy levels above 60% are generally regarded as acceptable (Hariyono et al. 2023).

Among the tested algorithms, Random Forest consistently demonstrated superior performance across all evaluation metrics. Confidence interval analysis derived from non-parametric bootstrapping indicates high classification reliability for both Random Forest and CART, whereas SVM exhibited greater uncertainty. Pairwise comparisons using McNemar's test further confirmed that Random Forest significantly outperformed both CART and SVM, and that CART also performed better than SVM. These findings statistically validate the robustness of the Random Forest classifier and align with previous studies emphasizing the strong generalization capability of ensemble-based methods in heterogeneous tropical environments (Zafari et al. 2019; Chowdhury 2024; Zafar et al. 2024). Similar conclusions have been reported in earlier studies demonstrating the effectiveness of ensemble classifiers under complex landscape conditions (Azedou et al. 2025).

Despite the generally high overall accuracies, class-level performance varied substantially among land-cover types, reflecting the complex landscape structure of Mount Argapura (Manyothwane and Mengistu 2025). Forest-related classes, particularly Natural Forest and Plantation Forest, were consistently classified with high producer's and user's accuracy under CART and Random Forest, indicating the strong capability of tree-based algorithms to capture forest dominance in mountainous tropical environments (Brito et al. 2025). In contrast, Plantation Estate and Dryland Agriculture showed markedly lower classification performance under SVM, suggesting significant confusion between managed plantation systems and surrounding forest or agricultural mosaics (Tan et al. 2024).

Misclassification among Plantation Estates, forests, and agricultural land is largely attributable to spectral similarity and phenological overlap between plantation canopies and Natural Forest structures, particularly where mature plantation stands exhibit dense canopy cover resembling Natural Forests (Huang et al. 2020). Seasonal vegetation dynamics, including leaf flushing and senescence, further reduce spectral separability between forest and non-forest

classes, increasing omission and commission errors, especially for margin-based classifiers such as SVM (Surasinghe et al. 2025). Moreover, the pronounced topographic complexity of Mount Argapura characterized by steep slopes and elevation gradients introduces illumination differences and shadow effects that alter spectral reflectance patterns and exacerbate classification uncertainty among spectrally similar land-cover classes (Buchner et al. 2020). Overall, the observed confusion patterns realistically represent the heterogeneous forest-agriculture transition zones of Mount Argapura, underscoring the suitability of ensemble-based approaches for forest mapping in complex mountainous landscapes (Wang et al. 2022)

Table 5 presents the total area and proportional coverage of each land-cover class derived from the Random Forest classification. Plantation Forest occupies the largest area, followed by Natural Forest and Plantation Estate, while Dryland Agriculture, Open Land, Settlements, and Water Bodies together account for a relatively small proportion of the landscape. These results indicate that Mount Argapura remains predominantly forested, although the substantial extent of plantation-related land cover reflects significant human modification of natural vegetation. This pattern suggests increasing anthropogenic pressure and ongoing land-use conversion, which may threaten ecological integrity if not managed sustainably (Alemayehu et al. 2024). The classified land-cover map reveals a clear spatial differentiation between forest and non-forest classes across Mount Argapura. Natural Forests are predominantly distributed in higher-elevation mountainous areas and form relatively contiguous patches, whereas Plantation Forests are mainly located in transitional zones surrounding Natural Forest areas. In contrast, non-forest classes such as Dryland Agriculture, Plantation Estates, and Settlements are concentrated in lower-elevation areas and along accessible valleys, reflecting accessibility-driven land-use patterns typical of mountainous tropical regions (Chidodo et al. 2025).

Visual inspection of the classified maps indicates that the Random Forest and SVM outputs exhibit spatial patterns closely resembling the reference basemap, whereas the CART-derived map appears more fragmented despite relatively high overall accuracy and Kappa values. This contrast reflects algorithmic differences: ensemble-based methods such as Random Forest and margin-based approaches such as SVM tend to generate more spatially coherent maps by reducing sensitivity to noise and outliers, while CART, which relies on a single decision tree, is more sensitive to threshold selection and training data distribution, often producing blocky or discontinuous boundaries (Al Farikhi and Pramono 2023). Because traditional accuracy metrics, including overall accuracy and Kappa, do not capture spatial allocation errors, visual and spatial assessments remain essential complements to pixel-based evaluation (Pontius et al. 2025).

The comparison between the classification map produced in this study and the MoEF map reveals differences in the extent of forest and vegetated land cover. The classification results indicate a higher proportion of plantation-related landscapes, whereas the MoEF map shows a relatively larger extent of Natural Forest cover within the study area. This difference occurs because the MoEF land-cover map is produced at a national scale, whereas the map generated in this study is developed at a local scale, allowing more detailed and accurate representation of site-specific land-cover conditions (Aldiansyah and Saputra 2022). These results are consistent with previous studies reporting that global-scale land-cover maps differ from locally derived maps in terms of mapping approaches and classification methods (Fonte et al. 2024). Global land-cover products have also been shown to exhibit significant classification differences when compared with regional mapping due to variations in spatial resolution and classification techniques (Bie et al. 2023). Furthermore, global land-cover datasets often require local adjustment, as variations in topography and landscape heterogeneity can lead to discrepancies between global and locally derived classifications (Aryal et al. 2023).

Implications for forest management

The availability of an accurate and up-to-date land-cover map for Mount Argapura provides significant benefits for both scientific research and practical forest management. This spatial dataset serves as a critical baseline for a wide range of environmental modelling applications, enabling researchers to quantify ecological processes with higher precision. Specifically, it facilitates the assessment of aboveground biomass and carbon stocks, which are vital for climate change mitigation strategies and carbon accounting (Sumarga et al. 2020). In the field of conservation biology, such maps are indispensable for habitat suitability and species distribution modelling (Siddiq et al. 2023). Accurate land-cover data also enhances disaster risk management by improving the accuracy of wildfire risk predictions (Sumarga 2017). In the field of hydrological modelling, land cover map provides important vegetation parameters required for a wide range of analysis, including soil erosion estimation (Moreno-Pájaro et al. 2025).

From a management perspective this land-cover map directly supports conservation initiatives in the Mount Argapura ecosystem by providing a spatial framework for protecting biodiversity and forest ecosystem services. Specifically, the map offers essential guidance for BKSDA and Perum Perhutani in managing the conservation, protection and production forests in the Mount Argapura region. For BKSDA, the availability of an accurate land-cover map serves as an important input for ensuring the long-term persistence of biodiversity, particularly in natural forest in the Iyang Highlands Wildlife Reserve. It provides a spatial inventory of existing ecosystems and detects forest degradation evidences such as illegal encroachment. By providing a clear picture of habitat fragmentation, this map enables the strategic allocation of limited resources toward restoration efforts in degraded areas. This map also facilitates BKSDA to evaluate the existing zonation and informs the strategic allocation of buffer zones by

analysing current land-cover and land-use patterns surrounding the wildlife reserve.

For Perum Perhutani, which manages both production and protection forests, the land cover map provides a reference for monitoring forest growth and degradation, and planning sustainable forest management. In the management of protection forests specifically designated for hydrological functions, an accurate land-cover map is a fundamental requirement for maintaining water yield and soil stability. This map allows Perum Perhutani to identify the spatial extent of critical recharge zones, ensuring that forest density and structure are sufficient to facilitate groundwater infiltration and minimize surface runoff. By monitoring vegetation cover, Perum Perhutani can determine areas where degradation might trigger flash floods or sedimentation in downstream reservoirs, and taking adequate intervention to restore forest cover and preserve the vital water services. In production forest management, one of the primary benefits of accurate land-cover mapping for Perum Perhutani is its utility in evaluating and planning agroforestry initiatives. This map provides essential data on the spatial distribution and patterns of agricultural land adjacent to the forest, identifying high-priority areas for agroforestry development. Such strategic planning fosters synergy between sustainable forest production and community empowerment, ensuring ecological and social harmony.

In conclusion, this study shows that RF outperforms CART and SVM in mapping land cover in the complex mountainous landscape of Mount Argapura, East Java, confirming its suitability for forestry-oriented remote sensing by accurately delineating key forest and non-forest classes, particularly natural and Plantation Forests. The validated Landsat 8/9 land-cover map provides a reliable baseline for forest monitoring, biodiversity conservation, and carbon stock assessment by BKSDA and Perhutani. The improvement from conventional to area-adjusted overall accuracy further highlights that design-based, area-weighted validation produces more unbiased and statistically robust estimates, strengthening its relevance for carbon accounting, REDD+, and national greenhouse gas monitoring. This spatial information supports the identification of forest-non-forest transition zones and evidence-based land-use planning, while future research should incorporate multi-temporal and higher-resolution or multi-sensor data to improve detection of fine-scale forest dynamics and reduce classification uncertainty.

ACKNOWLEDGEMENTS

The authors thank to the School of Life Sciences and Technology, Institut Teknologi Bandung, Indonesia, for technical support. Special appreciation is also extended to Mr. Ario Bhirowo, S.Hut from Hylobates Awara Foundation and Mr. Mohammad Thoha Zulkarnaen, M.Si from Nusantara Green Initiative for their support in remote sensing training. This research was supported by Mr. Kasraji, S.Hut through the HiFa Foundation, a private foundation that provides support for education. The authors declare no conflict of interest.

REFERENCES

Al Farikhi F, Pramono RWD. 2023. Perbandingan algoritma Classification and Regression Tree (CART) dan Random Forest (RF) untuk klasifikasi penggunaan lahan pada Google Earth Engine. Jurnal Spatial Wahana Komunikasi dan Informasi Geografi 23 (2): 170-179. https://doi.org/10.21009/spatial.232.09. [Indonesian]

Alcaras E, Costantino D, Guastaferro F, Parente C, Pepe M. 2022. Normalized Burn Ratio Plus (NBR+): A new index for Sentinel-2 imagery. Remote Sens 14 (7): 1727. https://doi.org/10.3390/rs14071727.

Aldiansyah S, Saputra RA. 2022. Comparison of machine learning algorithms for land use and land cover analysis using Google Earth Engine (case study: Wanggu Watershed). Intl J Remote Sens Earth Sci 19 (2): 197-210. https://doi.org/10.30536/ijreses.v19i2.13716.

Alemayehu B, Suarez-Minguez J, Rosette J. 2024. The implications of Plantation Forest-driven land use/land cover changes for ecosystem service values in the Northwestern highlands of Ethiopia. Remote Sens 16 (22): 4159. https://doi.org/10.3390/rs16224159.

Ali U, Esau TJ, Farooque AA, Zaman QU, Abbas F, Bilodeau MF. 2022. Limiting the collection of ground truth data for land use and land cover maps with machine learning algorithms. ISPRS Intl J Geo-Inf 11 (6): 333. https://doi.org/10.3390/ijgi11060333.

Amin G, Imtiaz I, Haroon E, Saqib NUS, Shahzad MI, Nazeer M. 2024. Assessment of machine learning algorithms for land cover classification in a complex mountainous landscape. J Geovis Spatial Anal 8 (2): 34. https://doi.org/10.1007/s41651-024-00195-z.

Anderson JRA. 1976. Land Use and Land Cover Classification System for Use with Remote Sensor Data. [Professional Paper]. US Geological Survey, Virginia. https://doi.org/10.3133/pp964.

Aryal K, Apan A, Maraseni T. 2023. Comparing global and local land cover maps for ecosystem management in the Himalayas. Remote Sens Appl Soc Environ 30: 100952. https://doi.org/10.1016/j.rsase.2023.100952.

Azedou A, Amine A, Kisekka I, Lahssini S. 2025. Genetic algorithm optimization of ensemble learning approach for improved land cover and land use mapping: Application to Talassemtane National Park. Ecol Indic 177: 113776. https://doi.org/10.1016/j.ecolind.2025.113776.

Biah I, Azihou AF, Guendehou S, Sinsin B. 2024. Land use/land cover change and carbon footprint in tropical ecosystems in Benin, West Africa. Tree For People 15: 100488. https://doi.org/10.1016/j.tfp.2023.100488.

Bie Q, Shi Y, Li X, Wang Y. 2023. Contrastive analysis and accuracy assessment of three global 30 m land cover maps circa 2020 in arid land. Sustainability 15 (1): 741. https://doi.org/10.3390/su15010741.

Bimaprawira AK, Rejeki HA. 2021. Relationship of rainfall periodicity in coastal and mountain areas of East Java Province with global and regional scale weather variability. Jurnal Sains dan Teknologi Modifikasi Cuaca 22 (2): 51-59. https://doi.org/10.29122/jstmc.v22i2.4422. [Indonesian]

Boer R, Anwar S, Margono BA et al. 2022. National Forest Reference Level for Deforestation, Forest Degradation, and Enhancement of Forest Carbon Stock. FREL Indonesia, Jakarta. [Indonesian]

Bogale T, Degefa S, Dalle G, Abebe G. 2025. Machine learning-based analysis of land use and land cover trends in southeastern Ethiopia using Google Earth Engine. Discov Sustain 6 (1): 878. https://doi.org/10.1007/s43621-025-01709-5.

Bragagnolo L, da Silva RV, Grzybowski JMV. 2021. Amazon forest cover change mapping based on semantic segmentation by U-Nets. Ecol Inform 62: 101279. https://doi.org/10.1016/j.ecoinf.2021.101279.

Brito CS dos S, Beltrão NES, Pimenta LB, de Jesus NCC. 2025. Performance of random forest and CART algorithms in land-use and land-cover classification on Cotijuba Island (PA) from 1989 to 2023. Rev Gest Soc Ambient 19 (12): e014093. https://doi.org/10.24857/rgsa.v19n12-048.

Buchner J, Yin H, Frantz D, Kuemmerle T, Askerov E, Bakuradze T, Bleyhl B, Elizbarashvili N, Komarova A, Lewińska KE, Rizayeva A, Sayadyan H, Tan B, Tepanosyan G, Zazanashvili N, Radeloff VC.

2020. Land-cover change in the Caucasus Mountains since 1987 based on the topographic correction of multi-temporal Landsat composites. Remote Sens Environ 248: 111967. https://doi.org/10.1016/j.rse.2020.111967.

Buthelezi MNM, Lottering RT, Peerbhay KY, Mutanga O. 2024. Predicting land use and land cover change dynamics in the eThekwini Municipality: A machine learning approach with Landsat imagery. J Spat Sci 69 (4): 1241-1263. https://doi.org/10.1080/14498596.2024.2378362.

Carletta J. 1996. Assessing agreement on classification tasks: The kappa statistic. Comput Linguist 22 (2): 249-254.

Cheng KS, Ling JY, Lin TW, Liu YT, Shen YC, Kono Y. 2021. Quantifying uncertainty in land-use/land-cover classification accuracy: A stochastic simulation approach. Front Environ Sci 9: 628214. https://doi.org/10.3389/fenvs.2021.628214.

Chidodo S, Zhang L, Zarei A, Feger KH. 2025. Remote sensing-based assessment of four decades of land use/land cover change in the Sigi River Watershed, East Usambara Mountains, Tanzania. Front Remote Sens 6: 1594331. https://doi.org/10.3389/frsen.2025.1594331.

Chowdhury MS. 2024. Comparison of accuracy and reliability of random forest, support vector machine, artificial neural network and maximum likelihood method in land use/cover classification of urban setting. Environ Chall 14: 100800. https://doi.org/10.1016/j.envc.2023.100800.

Congalton RG, Green K. 2005. Assessing the Accuracy of Remotely Sensed Data: Principles and Practices. 2nd Edition, CRC Press, Taylor & Francis Group, London.

Demirović E, Lukina A, Hebrard E, Chan J, Bailey J, Leckie C, Ramamohanarao K, Stuckey PJ. 2022. MurTree: Optimal decision trees via dynamic programming and search. J Mach Learn Res 23 (26): 1-47.

Dietz J, Treydte AC, Lippe M. 2023. Exploring the future of Kafue National Park, Zambia: Scenario-based land use and land cover modelling to understand drivers and impacts of deforestation. Land Use Policy 126: 106535. https://doi.org/10.1016/j.landusepol.2023.106535.

Esri. 2025. ArcGIS Pro Personal Use. Esri, Redlands, California. https://www.esri.com/.

Fonte CC, Duarte D, Jesus I, Costa H, Benevides P, Moreira F, Caetano M. 2024. Accuracy assessment and comparison of national, European and global land use land cover maps at the national scale: Case study Portugal. Remote Sens 16 (9): 1504. https://doi.org/10.3390/rs16091504.

Foody GM. 2020. Explaining the unsuitability of the kappa coefficient in the assessment and comparison of the accuracy of thematic maps obtained by image classification. Remote Sens Environ 239: 111630. https://doi.org/10.1016/j.rse.2019.111630.

Google Developers. 2025. Landsat. Mountain View, California. https://developers.google.com/earth-engine/datasets/catalog/landsat.

Guarderas P, Smith F, Dufrene M. 2022. Land use and land cover change in a tropical mountain landscape of northern Ecuador: Altitudinal patterns and driving forces. PLoS One 17 (7): e0260191. https://doi.org/10.1371/journal.pone.0260191.

Hanum U, Dianti, Safitri RN, Pratiwi VMR, Hermawan WG, Indrawan M, Setyawan AD. 2024. Ecological change detection in PT. Semen Gresik Rembang, Indonesia (limestone mining) activities between 2016 to 2022. Intl J Trop Drylands 8: 59-68.https://doi.org/10.13057/tropdrylands/t080201.

Hariyono MI, Rokhmatulloh, Dewi RS. 2023. Land use and land cover (LULC) classification with machine learning approach using orthophoto data. Majalah Ilmiah Globe 25 (1): 87-96. [Indonesian]

Harmoko J, Munibah K, Ardiansyah M. 2025. Klasifikasi penutupan/penggunaan lahan dari citra Landsat 8 dengan pendekatan random forest dan support vector machine di Kabupaten Sumedang, Jawa Barat. Jurnal Ilmu Tanah dan Lingkungan 27 (1): 24-31. https://doi.org/10.29244/jitl.27.1.24-31. [Indonesian]

Huang C, Zhang C, He Y, Liu Q, Li H, Su F, Liu G, Bridhikitti A. 2020. Land cover mapping in cloud-prone tropical areas using Sentinel-2 data: Integrating spectral features with NDVI temporal dynamics. Remote Sens 12 (7): 1163. https://doi.org/10.3390/rs12071163.

Islam MY, Nasher NMR, Karim KHR, Rashid KJ. 2023. Quantifying forest land-use changes using remote-sensing and CA-ANN model of Madhupur Sal Forests, Bangladesh. Heliyon 9 (5): e15617. https://doi.org/10.1016/j.heliyon.2023.e15617.

Jozdani SE, Johnson BA, Chen D. 2019. Comparing deep neural networks, ensemble classifiers, and support vector machine algorithms for object-based urban land use/land cover classification. Remote Sens 11 (14): 1713. https://doi.org/10.3390/rs11141713.

Kementerian Lingkungan Hidup dan Kehutanan (KLHK). 2022. Kementerian Lingkungan Hidup dan Kehutanan Republik Indonesia menuju FOLU Net Sink 2030. Kementerian Lingkungan Hidup dan Kehutanan, Jakarta. [Indonesian]

Landis JR, Koch GG. 1977. The measurement of observer agreement for categorical data. Biometrics 33 (1): 159-174. https://doi.org/10.2307/2529310.

Lemenkova P. 2024. Support vector machine algorithm for mapping land cover dynamics in Senegal, West Africa, using Earth observation data. Earth 5 (3): 420-462. https://doi.org/10.3390/earth5030024.

Mahmoud MI, Campbell MJ, Sloan S, Alamgir M, Laurance WF. 2020. Land-cover change threatens tropical forests and biodiversity in the Littoral Region, Cameroon. Oryx 54 (6): 882-891. https://doi.org/10.1017/S0030605318000881.

Manyothwane T, Mengistu TG. 2025. Challenging global generalizations: Superior land cover mapping in Botswana with a locally trained transformer model. Front Remote Sens 6: 1654692. https://doi.org/10.3389/frsen.2025.1654692.

Melichar M, Didan K, Barreto-Muñoz A, Duberstein JN, Jiménez Hernández E, Crimmins T, Li H, Traphagen M, Thomas KA, Nagler PL. 2023. Random forest classification of multitemporal Landsat 8 spectral data and phenology metrics for land cover mapping in the Sonoran and Mojave Deserts. Remote Sens 15 (5): 1266. https://doi.org/10.3390/rs15051266.

Moreno-Pájaro ÁM, Osorio-Gastelbondo A, Moreno-Egel DA, Coronado-Hernández OE, Narváez-Cuadro MA, Saba M, Arrieta-Pastrana A. 2025. Hydrological modelling and remote sensing for assessing the impact of vegetation cover changes. Hydrology 12 (5): 107. https://doi.org/10.3390/hydrology12050107.

Muhamad D, Okubo S, Harashina K, Parikesit, Gunawan B, Takeuchi K. 2014. Living close to forests enhances people's perception of ecosystem services in a forest-agricultural landscape of West Java, Indonesia. Ecosyst Serv 8: 197-206. https://doi.org/10.1016/j.ecoser.2014.04.003.

Ouchra H, Belangour A, Erraissi A. 2023. Machine learning algorithms for satellite image classification using Google Earth Engine and Landsat satellite data: Morocco case study. IEEE Acces 11: 71127-71142. https://doi.org/10.1109/ACCESS.2023.3293828.

Pontius Jr RG, Francis T, Millones M. 2025. A call to interpret disagreement components during classification assessment. Intl J Geogr Inf Sci 39 (7): 1373-1390. https://doi.org/10.1080/13658816.2025.2469830.

Ramezan CA, Warner TA, Maxwell AE. 2019. Evaluation of sampling and cross-validation tuning strategies for regional-scale machine learning classification. Remote Sens 11 (2): 185. https://doi.org/10.3390/rs11020185.

Rouse RWH, Haas JAW, Deering DW. 1974. Monitoring vegetation systems in the Great Plains with ERTS. Goddard Space Flight Center 3d ERTS-1 Symposium, 1, 309-317. NASA, Greenbelt, Maryland.

Roy DP, Kovalskyy V, Zhang HK, Vermote EF, Yan L, Kumar SS, Egorov A. 2016. Characterization of Landsat-7 to Landsat-8 reflective wavelength and normalized difference vegetation index continuity. Remote Sens Environ 185: 57-70. https://doi.org/10.1016/j.rse.2015.12.024.

Sari IL, Weston CJ, Newnham GJ, Volkova L. 2021. Assessing accuracy of land cover change maps derived from automated digital processing and visual interpretation in tropical forests in Indonesia. Remote Sens 13 (8): 1446. https://doi.org/10.3390/rs13081446.

Shah RK, Shah RK. 2023. Forest Cover Change Detection using Remote Sensing and GIS in Dibru-Saikhowa National Park, Assam: A Spatio-Temporal Study. Proc Natl Acad Sci India Sect B Biol Sci 93 (3): 559-564. https://doi.org/10.1007/s40011-023-01449-4.

Shahfahad, Talukdar S, Naikoo MW, Rahman A, Gagnon AS, Islam ARMT, Mosavi A. 2023. Comparative evaluation of operational land imager sensor on board Landsat 8 and Landsat 9 for land use land cover mapping over a heterogeneous landscape. Geocarto Intl 38 (1): 2152496. https://doi.org/10.1080/10106049.2022.2152496.

Shetty S, Gupta PK, Belgiu M, Srivastav SK. 2021. Assessing the effect of training sampling design on the performance of machine learning classifiers for land cover mapping using multi-temporal remote sensing data and Google Earth Engine. Remote Sens 13 (8): 1433. https://doi.org/10.3390/rs13081433.

Siddiq AM, Subchan W, Maulahila HI, Kholiq N. 2023. Habitat suitability model for banteng (*Bos javanicus*) in Meru Betiri National Park,

Indonesia. Biodiversitas 24 (2): 1296-1302. https://doi.org/10.13057/biodiv/d240272.

Slagter B, Fesenmyer K, Hethcoat M, Belair E, Ellis P, Kleinschroth F, Peña-Claros M, Herold M, Reiche J. 2024. Monitoring road development in Congo Basin forests with multi-sensor satellite imagery and deep learning. Remote Sens Environ 315: 114380. https://doi.org/10.1016/j.rse.2024.114380.

Sovann C, Tagesson T, Vestin P, Sakhoeun S, Kim S, Kok S, Olin S. 2025. Land-cover change alters stand structure, species diversity, leaf functional traits, and soil conditions in Cambodian tropical forests. Biogeosciences 22 (18): 4649-4677. https://doi.org/10.5194/bg-22-4649-2025.

Sumarga E, Nurudin N, Suwandhi I. 2020. Land-cover and elevation-based mapping of aboveground carbon in a tropical mixed-shrub forest area in West Java, Indonesia. Forests 11 (6): 636. https://doi.org/10.3390/F11060636.

Sumarga E. 2017. Spatial indicators for human activities may explain the 2015 fire hotspot distribution in Central Kalimantan, Indonesia. Trop Conserv Sci 10: 1-10. https://doi.org/10.1177/1940082917706168.

Surasinghe TD, Singh KK, Smart LS. 2025. Leveraging phenology to assess seasonal variations of plant communities for mapping dynamic ecosystems. Remote Sens 17 (10): 1778. https://doi.org/10.3390/rs17101778.

Tan YC, Duarte L, Teodoro AC. 2024. Comparative study of random forest and support vector machine for land cover classification and post-wildfire change detection. Land 13 (11): 1878. https://doi.org/10.3390/land13111878.

Tassi A, Vizzari M. 2020. Object-oriented LULC classification in Google Earth Engine combining SNIC, GLCM, and machine learning algorithms. Remote Sens 12 (22): 3776. https://doi.org/10.3390/rs12223776.

Tewabe D, Fentahun T. 2020. Assessing land use and land cover change detection using remote sensing in the Lake Tana Basin, Northwest Ethiopia. Cogent Environ Sci 6 (1): 1778998. https://doi.org/10.1080/23311843.2020.1778998.

Trisasongko BH, Panuju DR, Karyati NE, I'anatus Sholihah R. 2022. Comparison of machine learning models for land cover classification. Intl J Remote Sens Earth Sci 19 (1): 21-29. https://doi.org/10.30536/ijreses.v19i1.13781.

Valero MJA, Alzate ABE. 2019. Comparison of maximum likelihood, support vector machines, and random forest techniques in satellite images classification. Tecnura 23 (59): 13-26. https://doi.org/10.14483/22487638.14826.

Vatitsi K, Ioannidou N, Mirli A, Siachalou S, Kagalou I, Latinopoulos D, Mallinis G. 2023. LULC change effects on environmental quality and ecosystem services using EO data in two rural river basins in Thrace, Greece. Land 12 (6): 1140. https://doi.org/10.3390/land12061140.

Velastegui-Montoya A, Montalván-Burbano N, Peña-Villacreses G, de Lima A, Herrera-Franco G. 2022. Land use and land cover in tropical forest: Global research. Forests 13 (10): 1709. https://doi.org/10.3390/f13101709.

Wang Y, Liu H, Sang L, Wang J. 2022. Characterizing forest cover and landscape pattern using multi-source remote sensing data with ensemble learning. Remote Sens 14 (21): 5470. https://doi.org/10.3390/rs14215470.

Winkler K, Fuchs R, Rounsevell M, Herold M. 2021. Global land use changes are four times greater than previously estimated. Nat Commun 12 (1): 2501. https://doi.org/10.1038/s41467-021-22702-2.

Xu H, Sun H, Xu Z, Wang Y, Zhang T, Wu D, Gao JH. 2025. kNDMI: A kernel normalized difference moisture index for remote sensing of soil and vegetation moisture. Remote Sens Environ 319: 114621. https://doi.org/10.1016/j.rse.2025.114621.

Yousefi S, Mirzaee S, Almohamad H, Al Dughairi AA, Gomez C, Siamian N, Alrasheedi M, Abdo HG. 2022. Image classification and land cover mapping using Sentinel-2 imagery: Optimization of SVM parameters. Land 11 (7): 993. https://doi.org/10.3390/land11070993.

Yuh YG, Tracz W, Matthews HD, Turner SE. 2023. Application of machine learning approaches for land cover monitoring in Northern Cameroon. Ecol Inform 74: 101955. https://doi.org/10.1016/j.ecoinf.2022.101955.

Zafar Z, Zubair M, Zha Y, Fahd S, Ahmad Nadeem A. 2024. Performance assessment of machine learning algorithms for mapping of land use/land cover using remote sensing data. Egypt J Remote Sens Space Sci 27 (2): 216-226. https://doi.org/10.1016/j.ejrs.2024.03.003.

Zafari A, Zurita-Milla R, Izquierdo-Verdiguier E. 2019. Evaluating the performance of a random forest kernel for land cover classification. Remote Sens 11 (5): 575. https://doi.org/10.3390/rs11050575.